

AJ-A079 933

FOREIGN TECHNOLOGY DIV WRIGHT-PATTERSON AFB OH  
EXPERIMENTAL RESEARCH ON FLOW OPTIMIZATION IN LOW-SPEED WIND TU--ETC(U)  
JUL 79 S N SAVULESCU, V TOMA, G G GHEORGHIU

F/G 20/4

UNCLASSIFIED

FTD-ID(RS)T-0880-79

NL

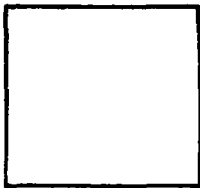
[ ]  
[ ]  
[ ]


END  
DATE  
FILMED  
2 - 80  
DDC

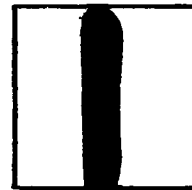
PHOTOGRAPH THIS SHEET

ADA 079933

DTIC ACCESSION NUMBER



LEVEL



INVENTORY

FTD-ID(RS)T-0880-79

DOCUMENT IDENTIFICATION

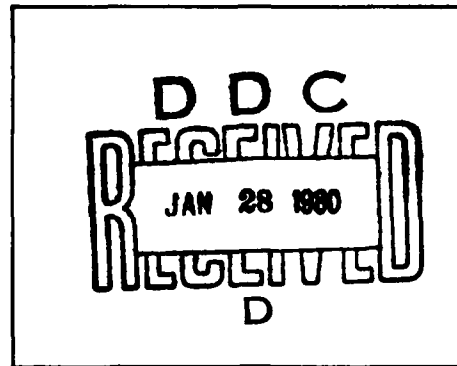
**DISTRIBUTION STATEMENT A**

Approved for public release;  
Distribution Unlimited

**DISTRIBUTION STATEMENT**

ACCESSION FOR	
NTIS	GRA&I
DTIC	TAB
UNANNOUNCED	
JUSTIFICATION	
BY	
DISTRIBUTION /	
AVAILABILITY CODES	
DIST	AVAIL AND/OR SPECIAL
A	

DISTRIBUTION STAMP



DATE ACCESSIONED

79 11 13 270

DATE RECEIVED IN DTIC

PHOTOGRAPH THIS SHEET AND RETURN TO DTIC-DDA-2

ADA 079933

# FOREIGN TECHNOLOGY DIVISION



EXPERIMENTAL RESEARCH ON FLOW OPTIMIZATION IN  
LOW-SPEED WIND TUNNELS

by

St. N. Săvulescu, V. Toma., Gh. Gh. Gheorghiu



Approved for public release;  
distribution unlimited.



## EDITED TRANSLATION

FTD-ID(RS)T-0880-79

25 July 1979

MICROFICHE NR:

*AD-79-C-000979*

EXPERIMENTAL RESEARCH ON FLOW OPTIMIZATION IN  
LOW-SPEED WIND TUNNELS

By: St. N. Săvulescu, V. Toma., Gh. Gh. Gheorghiu

English pages: 21

Source: Studii Si Cercetari De Mecanica Aplicata,  
Vol. 37, Nr. 2, March-April 1978, pp. 159-176.

Country of origin: Romania

Requester: FTD/TQTA

Approved for public release; distribution unlimited.

THIS TRANSLATION IS A RENDITION OF THE ORIGINAL FOREIGN TEXT WITHOUT ANY ANALYTICAL OR EDITORIAL COMMENT. STATEMENTS OR THEORIES ADVOCATED OR IMPLIED ARE THOSE OF THE SOURCE AND DO NOT NECESSARILY REFLECT THE POSITION OR OPINION OF THE FOREIGN TECHNOLOGY DIVISION.

PREPARED BY:

TRANSLATION DIVISION  
FOREIGN TECHNOLOGY DIVISION  
WP-AFB, OHIO.

FTD

-ID(RS)T-0880-79

Date 25 Jul 19 79

EXPERIMENTAL RESEARCH ON FLOW OPTIMIZATION IN  
LOW-SPEED WIND TUNNELS

St. N. Săvulescu, V. Toma., Gh. Gh. Gheorghiu  
IMFCA

The authors present their research on determining the optimal geometry, static pressure and velocity fields and the effect of perturbations in low speed wind tunnels (3-15 m/s), in which the flow is controlled by specific adjustment elements. The results could be used in designing subsonic wind tunnels.

1. Introduction

It is known that adjusting a low speed wind tunnel to respond to a wide variety of tests is long and difficult. The present work, for the particular case of Eolin wind tunnels, presents in a systematic fashion research undertaken with the following **objectives**:

--optimizing the aerodynamic circuit through modification of the fan chamber;

--optimization of the wind tunnel by making the fan intake aerodynamic;

--widening of the performance range of the wind tunnel by using special perturbators (to simulate bursts, atmospheric boundary layer, etc.);

--gathering of experimental data characteristic to the wind tunnel (cross-sectional velocity field, longitudinal pressure fields, etc.);

--calibration of the wind tunnel as a function of the combined effects of fans, perturbators and adjustment elements.

## 2. Modifications to the Aerodynamic Circuit of the Eolin CE4V Wind Tunnel

The following modifications were made: a segment with perturbators was introduced upstream of the experimental chamber, the fan chamber was enlarged by adding a parallelepipedic segment and the fan intake was aerodynamically designed.

Using a micromanometer, fluctuations were observed in the experimental chamber. This was attributed mainly to the inability of the fan chamber to dampen the fluctuations generated by the fans. To eliminate this, the chamber upstream of the fans was enlarged by 60% by adding a parallelepipedic segment as shown in Figure 1.

This addition has improved the flow in the experimental chamber. This was concluded by exploring the flow with a warm line. The operation of the fans was improved by aerodynamically designing the air intake. For this, profiled intake parts for each of the fans were built as shown in Figure 2. The effect of increasing the volume of the fan chamber is more important than that due to aerodynamically designing the fan intake. This is illustrated in Figures 3 and 4 in the form of the pressure distribution along the wind tunnel for two cases: with aerodynamic and nonaerodynamic intake, respectively 2 (Figure 3) and 4 (Figure 4) fans. There are slight differences between the two cases. This does not justify the aerodynamic design (difficult due to space requirements). There is a slight increase in the average velocity. This shows, for this kind of small axial fans with air intake from a large chamber, that profiling the fan intake is not an important factor in their performance.

Another change in the circuit consists in the introduction of two perturbing segments: one in front of the experimental chamber (closed experimental zone) the other upstream of the outgoing jet (open experimental zone). These are shown in Figure 1 together with their location in the aerodynamic circuit of the wind tunnel. The perturbing segment upstream of the experimental chamber offers five

possibilities of introducing of 300x300 perturbing frames: three vertical and two horizontal, which lengthens the experimental chamber by  $l_1 = 230$  mm. The second perturbing segment is a frame which allows the independent action of 40 blades situated on five axes. Its length is  $l_2 = 100$  m. Both perturbing segments, which introduce local losses, are movable, they can be taken in and out according to the needs.

### 3. Static Pressure Distribution along the Circuit

In this section the pressure distribution along the wind tunnel is presented. This in order to show the effects of working in various regimes: with 4 and 2 fans or fan and perturbing grid combinations. At the same time these distributions show the differences at the intakes along the contours of various sections, giving an indication on the local uniformity of the flow. Thus Figures 5a and 5b show the variation of coefficient  $C_p$  along the circuit for all the intakes and cases indicated.  $C_p$  is defined as  $C_p = \frac{P - P_a}{P_t - P_a}$

where  $P$  = local pressure (static intake);

$P_a$  = atmospheric pressure;

$P_t$  = total pressure in experimental chamber;

$P_{st}$  = static pressure at the wall of experimental chamber.

It can be seen that in the fan chamber the pressure is not uniformly distributed along the contours, locally there are complex and reverse flows. These are due to the interaction between the walls, the central flow and the flow in the vicinity of each fan. The non-uniformity of static pressure in a section is more pronounced for the case of 2 fans (Figure 5a) than for 4 fans (Figure 5b).

From these experiments regarding the distribution of static pressures it was concluded that in certain sections 4-6 intakes are necessary along the contour, whereas in other sections it can be limited to one or two.

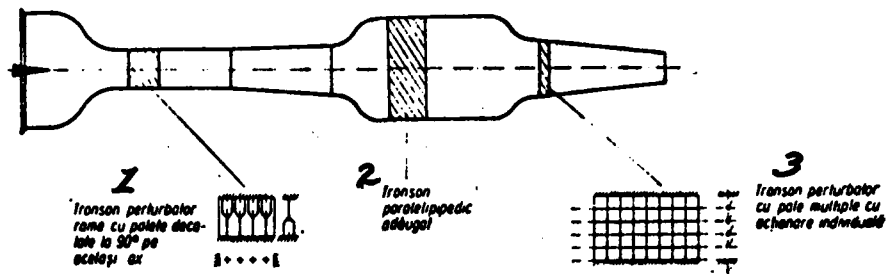


Figure 1

Key: 1 - Perturbing segment frames with blades at 90° on the same axis; 2 - Added parallelepipedic segment; 3 - Perturbing segment with multiple blades and independent acting

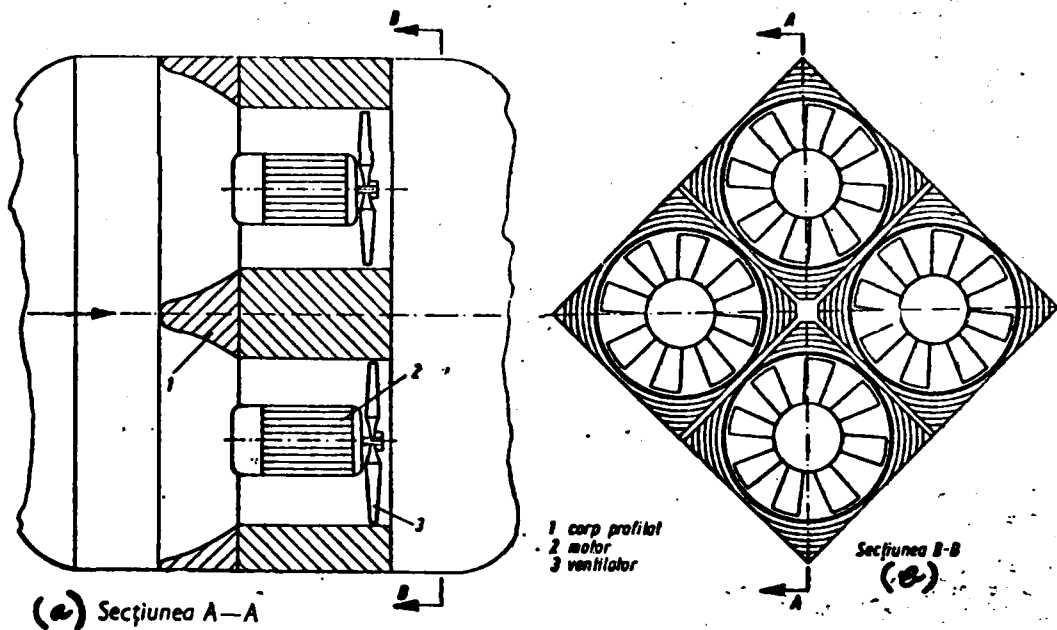


Figure 2

Key: (a) Section A-A; (b) Section B-B; 1 - profiled body; 2 - motor; 3 - fan

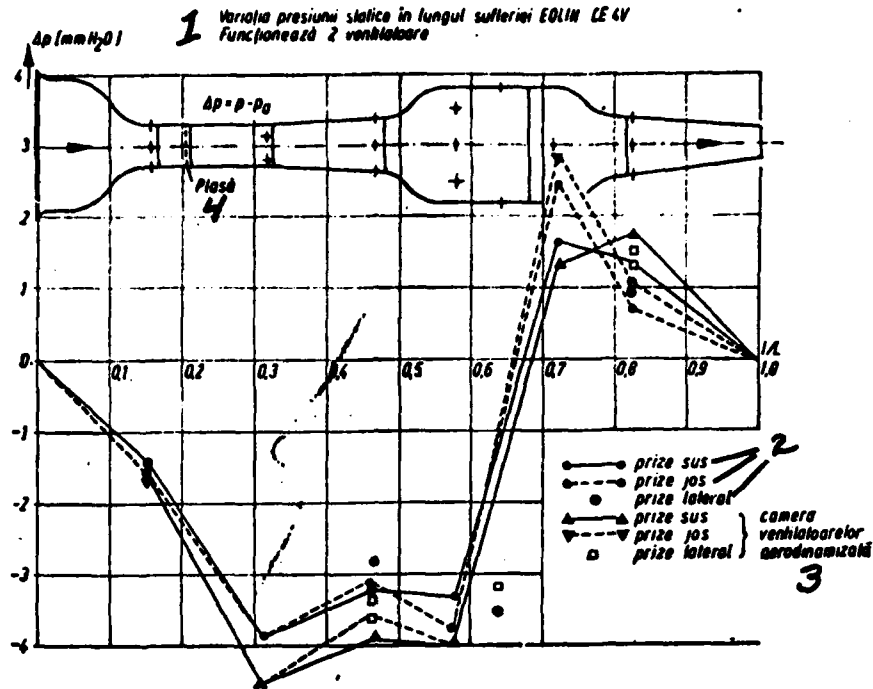


Figure 3

Key: 1 - Change in static pressure along Eolin CE4V wind tunnel; 2 - fans working; 3 - aerodynamic fan chamber; 4 - net

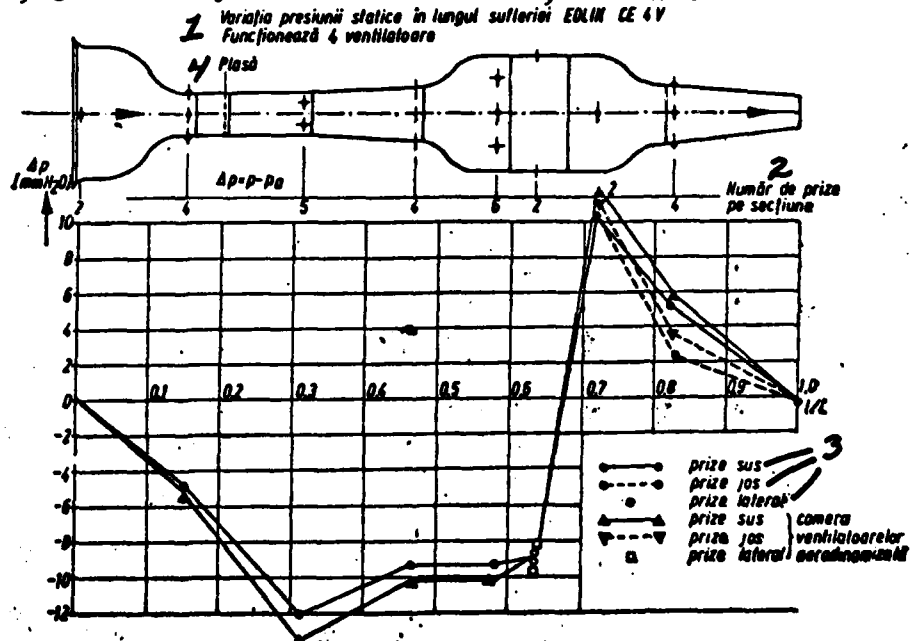


Figure 4

Key: 1 - Static pressure along Eolin CE4V wind tunnel; 4 fans working; 2 - number of intakes per section; 3 - intakes up, intakes down, intakes on side; 4 - net

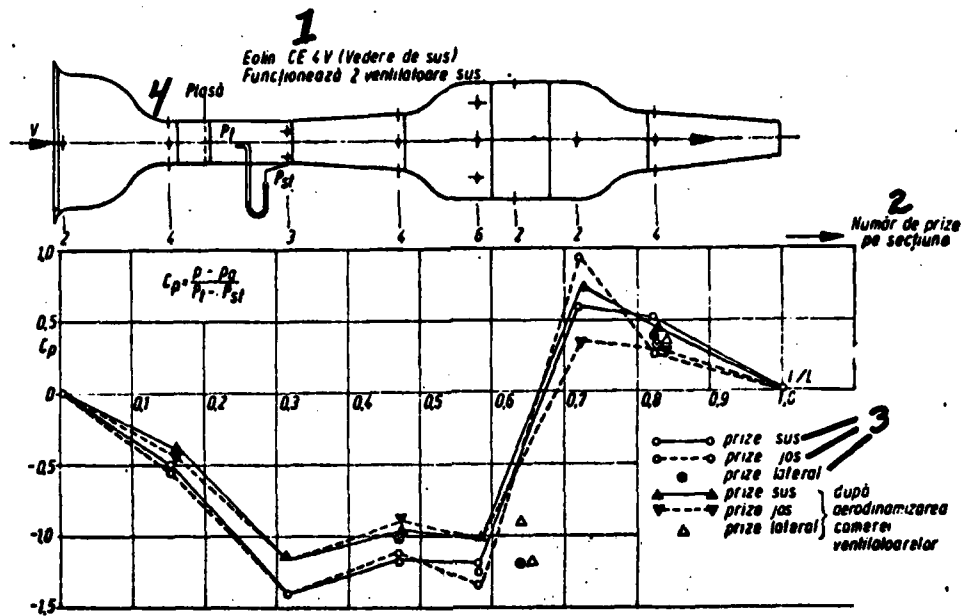


Figure 5a

Key: 1 - Eolin CE4V view from top 2 fans at top working; 2 - number of intakes per section; 3 - intakes up, intakes down, intakes on side; 4 - net

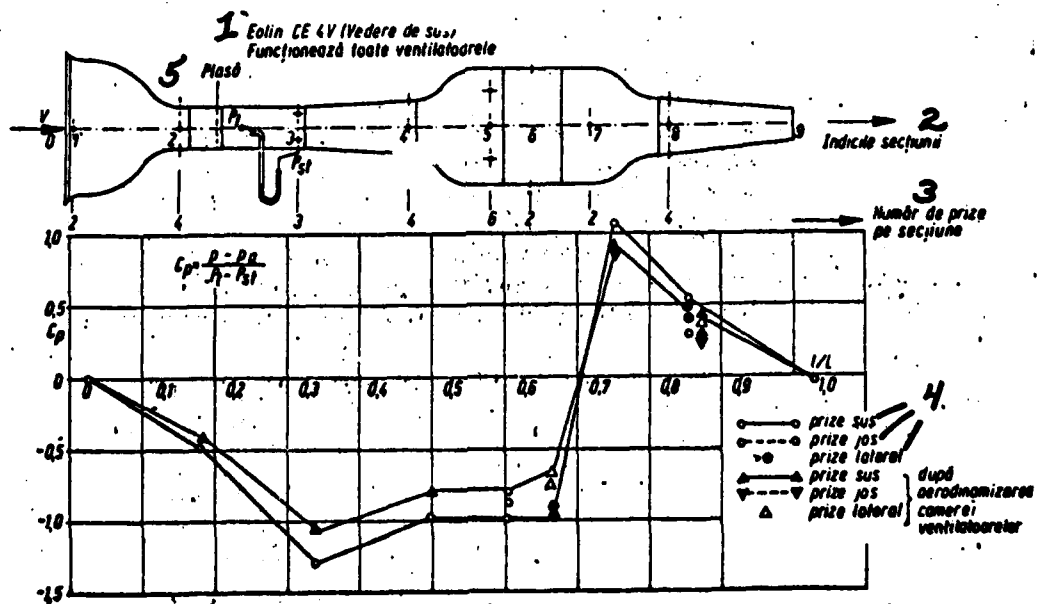


Figure 5b

Key: 1 - Eolin CE4V top view all fans working; 2 - section index; 3 - number of intakes per section; 4 - intakes up, intakes down, intakes on side; 5 - net

The distribution of static pressures along the wind tunnel represents the combined effects of the variation in potential pressure (Bernoulli eg.) and friction at the walls (boundary layer). For low speeds and large variations in cross-section these two effects are difficult to separate. Following is an analysis of the longitudinal pressure distribution, based on correcting the potential changes with boundary layer effects.

Let us consider a segment of square cross-section which varies with X (along the axis of the wind tunnel) (Figure 6). On the walls there is a boundary layer attached to the walls and without secondary corner flows.

The continuity equation for 1/4 of cross-section OAB between sections (1) and (2) is:

$$\frac{1}{4} (a_1 - 2\delta_1)^2 U_1 + (a_1 - 2\delta_1)\Psi_{s_1} = \frac{1}{4} (a_2 - 2\delta_2)^2 U_2 + (a_2 - 2\delta_2)\Psi_{s_2} \quad (3.1)$$

where

$$\Psi_{s_1} = \int_0^{a_1} U_1 dy, \quad \Psi_{s_2} = \int_0^{a_2} U_2 dy,$$

On the axis the Bernoulli equation is:

$$P_1 + \rho/2 U_1^2 = P_2 + \rho/2 U_2^2 \quad (3.2)$$

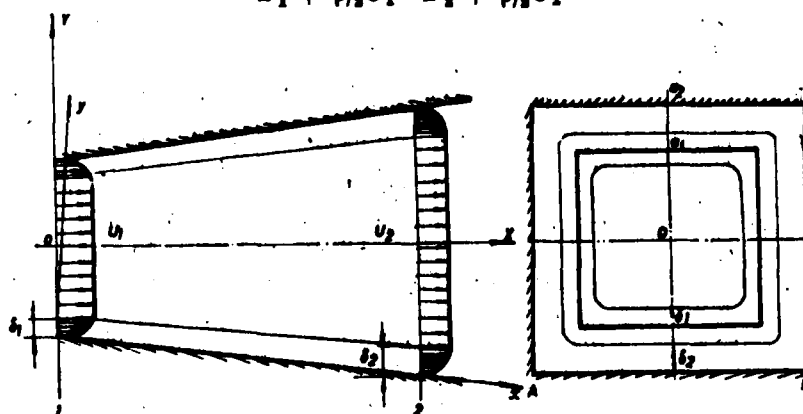


Figure 6

where

$$\begin{aligned} P_1 &= p_{o_1} + \rho/2 (u_1^2 - v_1^2) \\ P_2 &= p_{o_2} + \rho/2 (u_2^2 - v_2^2) \end{aligned} \quad (3.3)$$

$P_{w1}$  and  $P_{w2}$  are the static pressures at the wall at Section (1) and respectively (2), and  $u'$  and  $v'$  the velocity fluctuations in the two dimensional turbulent boundary layer at the wall. Referring to Section (1) we obtain by combining equations (3.1) and (3.2)

$$\Delta p_r = p_{w1} - p_{w2} [ (= \rho_{12}(u_1'^2 - u_2'^2) - (v_1'^2 - v_2'^2)) ] + \\ + \rho_{12} U_1^2 \left\{ 1 - \left[ \frac{(a_1 - 2\delta_1)^2}{(a_2 - 2\delta_2)^2} + \frac{4}{U_1} \cdot \frac{\Psi_{\delta_1}(a - 2\delta_1) - (a_2 - 2\delta_2)\Psi_{\delta_2}}{(a_2 - 2\delta_2)^2} \right]^2 \right\}$$

where the effects due to the turbulent boundary layer on the walls are included in the fluctuation term and in the curly brackets  $\delta_1, \delta_2, \Psi_{\delta_1}, \Psi_{\delta_2}$ . In the ideal case (no boundary layer):

thus

$$u', v' \sim 0 \quad \delta \sim 0, \Psi_{\delta} \sim 0,$$

$$\Delta p_i = (p_{w1} - p_{w2})_i = \frac{\rho}{2} U_1^2 \left[ 1 - \frac{a_1^4}{a_2^4} \right] \quad (3.4)$$

which is the ideal pressure change between Sections (1) and (2).

The actual difference in static pressure between Sections (1) and (2) can be written as

$$\Delta p_r = \Delta p_i + \frac{\rho}{2} [(u_1'^2 - u_2'^2) - (v_1'^2 - v_2'^2)] + \\ + \frac{\rho}{2} U_1^2 \frac{a_1^4}{a_2^4} \left\{ 1 - \left[ \frac{\left(1 - 2\frac{\delta_1}{a_1}\right)^2 + \frac{4}{U_1} \left[ \frac{\Psi_{\delta_1} \left(1 - 2\frac{\delta_1}{a_1}\right) - \frac{\Psi_{\delta_2} \left(\frac{a_2}{a_1} - \frac{\delta_2}{a_1}\right)}{a_1} \right]}{\left(1 - 2\frac{\delta_2}{a_2}\right)^2} \right]^2 \right\} \quad (3.5)$$

Equation (3.5) can be applied for a segment without local resistances (grids, perturbators) or sudden variations in cross-section (widening, narrowing). If these are present the development of the boundary layer is completely different. For example, equation (3.5) can be applied to the funnel in front of the fan chamber, which for  $\frac{\rho}{2} V_1^2 \cong 9,632 \text{ mm H}_2\text{O}$  column  $\text{H}_2\text{O}$  should convert speed into pressure with a gain of 6,364 mm  $\text{H}_2\text{O}$ . From the diagram in Figure 4 we obtain a gain of only 4 mm  $\text{H}_2\text{O}$ . This shows the effect of the fluctuation term and formation of boundary layer. These terms can be evaluated

from the theory of the turbulent boundary layer on the walls of the wind tunnel. The starting point is taken at the joining of the converging segment to the experimental chamber. Such an analysis is beyond the scope of this work though.

A first approximation estimate can be obtained as follows:

--the fluctuations terms are neglected, thus

$$(u_1'^2 - u_2'^2) - (v_1'^2 - v_2'^2) \cong 0,$$

--the speed profile in the boundary layer is determined experimentally, thus one obtains:

$$\Psi_{\delta_1} = \int_0^{\delta_1} U_{\max} dy, \quad \Psi_{\delta_2} = \int_0^{\delta_2} U_{\max} dy, \quad \text{for } \delta_1, \delta_2,$$

which allow equation (3.5) to be calculated.

In order to see why equation (3.5) is not applicable for sudden changes of cross-section, when the development of the boundary layer is abnormal and the main flow is substantially influenced by secondary flows, let us evaluate the change in pressure between the end section of the funnel (S4) and the section in front of the fans (S5) (See Figure 5b)

$$\Delta p_t = \frac{\rho}{2} U_1^2 \left(1 - \frac{a_4^2}{a_3^2}\right) = \left[\frac{\rho}{2} U_1^2 + (p_3 - p_4)\right] \left[1 - \frac{a_4^2}{a_3^2}\right]$$

$$\Delta p_t = (9,632 - 3) \left(1 - \frac{0,39^4}{0,8^4}\right) \cong 6 \text{ mm H}_2\text{O}.$$

From these 6 mm H<sub>2</sub>O, which should have been reconverted by the change in cross-section, one can see that only less than 1 mm H<sub>2</sub>O has been reconverted. This illustrates the disastrous effect of the sudden increase in cross-section on recovering the loss of pressure.

Appreciable variations in pressure, along the tube, are obtained by introducing a grid G made out of scotch tape 20 mm wide and placed at the end of the funnel. The unit of the grid is 65x65, and the degree of permeability  $\gamma = \frac{65 \times 65}{85 \times 85} = 0.585$ . Figure 7 shows

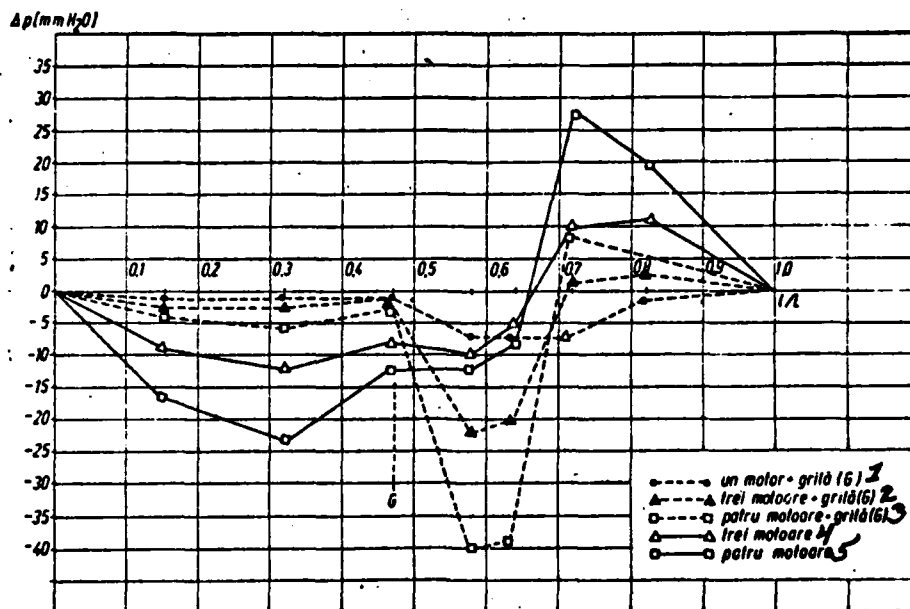


Figure 7

Key: 1 - one motor + grid (G); 2 - 3 motors + grid (G); 3 - 4 motors + grid (G); 4 - 3 motors; 5 - 4 motors

the jump in pressure (decrease) introduced by this local resistance for all the regimes of the wind tunnel (1, 3, 4 motors). Using these diagrams the local coefficient of loss of pressure can be obtained from the formula

$$C_x = \frac{(P_4 - P_5)_{\text{grid}} - (P_4 - P_5)_{\text{without grid}}}{\frac{\rho}{2} V_4^2 \text{ with grid}}$$

One obtains the following:

Regime	1 motor	3 motors	4 motors
$V_4$ m/s	2.4	3.9	5.82
$C_x$	14.4	20.5	17.4

One can see that the simultaneous action of more than one fan in the presence of the grid and sudden change of cross-section leads to large values of  $C_x$ , caused both by the small speeds of flow and

its local complexity. Nevertheless the introduction of a local resistance, such as a grid or perturbator, with a local loss of load  $\Delta p_{local} < 6$  mm does not affect the efficiency of the installation.

#### 4. The effects of the Adjustment Systems and Perturbators

Eolin wind tunnels have the following systems of acting on the flow characteristics:

A. Adjusting systems: Grid of obturator blades in front of motor chamber ( $G_p$ ), side doors to the motor chamber, separate operation of the motors.

B. Perturbing systems:  $P_1$  in front of the experimental chamber,  $P_2$  upstream of the convergent segment which furnishes the outgoing jet.

A. By using the adjusting systems controlled changes of the average characteristics of the flow, in particular speed in the experimental chamber and in the outgoing jet, can be obtained. One can act on three elements to obtain the desired speed and a good flow: side doors with variable opening grid with adjustable blades  $G_p$  and fans. Thus the side doors to the fan chamber maintain their working regime at optimum performance, even when the flow capacity through the experimental chamber is very small. Also the grid with blades ( $G_p$ ) in front of the fan chamber introduces a symmetrical resistance in the circuit downstream from the experimental chamber, in order not to additionally distort the flow structure.

We have thus obtained in the experimental chamber a range of speeds of 2-20 m/s in very small steps (0.5 m/s). In the outgoing jet the range of speeds is 5-15 m/s in fine steps (1 m/s).

B. The perturbing systems are utilized for controlled changes of the structure of the flow, such as degree of turbulence, speed profile and quasi laminar character of the average flow. Thus for the flow in the experimental chamber the perturbator  $P_1$  offers the

following possibilities:

--achieving a roughness which leads to an increase in the thickness of the boundary layer.

--mounting an obturator sieve-grid for turbulence, which leads to modification of the degree of turbulence of the flow.

--mounting a special obturator with blades, which allows obtaining three-dimensional speed profiles.

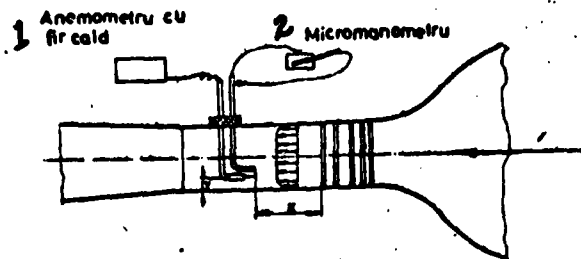
--mounting a perturbator with oscillating blades capable of producing a periodic change (in time) of the average flow.

For the outgoing jet, perturbator  $P_2$  allows mounting of a perturbing system with individually acted blades capable of achieving the desired speed profile.

Next we present some of the effects of these perturbators and adjusting systems: changes in the degree of turbulence, development of the boundary layer on the walls and speed profile in the experimental zone.

Degree of Turbulence (defined as  $T_u = \sqrt{\frac{\overline{u'^2}}{U}}$ ) is a decisive parameter for the structure of the flow. The wind tunnel offered the following results shown in Table 1 and the adjoining sketch.

Without the perturbator  $T_u = 0.37\%$ , with a passive grid and louvers at  $15^\circ$  the degree of turbulence is increased 20 times ( $T_u = 7.2\%$ ). Thus the range of turbulence in the experimental chamber is fairly wide. In the outgoing jet, due to the effect of perturbator  $P_2$ , one obtains a speed profile  $U(y)$  and correspondingly a distribution profile of the longitudinal turbulence shown in the diagrams (Figures 8-1, 8-2). Distributions  $\frac{\overline{u'^2}}{\overline{u'^2}}$  and  $\frac{U}{U_{\max}}$  are connected through an integral change of coordinates [1], [2].



Key: 1 - anemometer with warm flow; 2 - micromanometer;

TABLE 1

Regime	Perturbator	Measuring point x,y mm	Avg. speed U m/s	Degree of turbulence $\sqrt{u^2}/U\%$	Field uniformity of the degree of turbulence
4 fans	$P_0$ = without perturbator	x=310 y=140	19.9	0.37	homogeneous
4 fans	$P_1$ = plane passive grid	x=310 y=140	20.0	0.495	non-homogeneous
4 fans + compressor	$P_2$ = active grid with jets	x=310 y=140	20.1	0.55	non-homogeneous
4 fans	$P_3$ = passive grid with louvers at $15^\circ$	x=310 y=60	19.8	6.46	homogeneous
4 fans	$P_3$ = passive grid with louvers at $(15^\circ)$	x=310 y=140	20.4	7.20	homogeneous
4 fans + compressor	$P_4$ = active grid with jets and louvers at $15^\circ$	x=310 y=230	17.5	6.01	homogeneous

Development of the boundary layer on the wind tunnel walls.

In order to determine the usable (active) zone in the experimental chamber and to study the effect of roughness on the thickening of the boundary layer the speed profiles on the wind tunnel walls, at the sections indicated in Figure 8a, were measured.

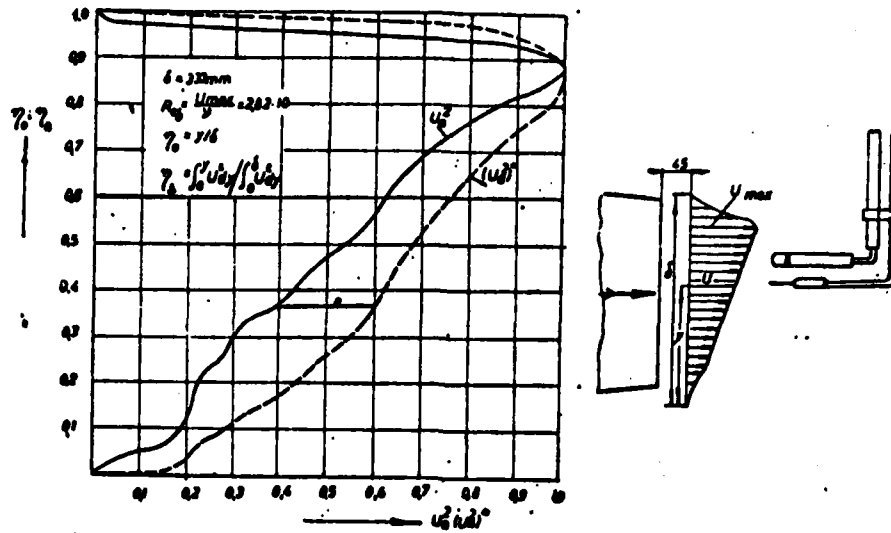


Figure 8-1

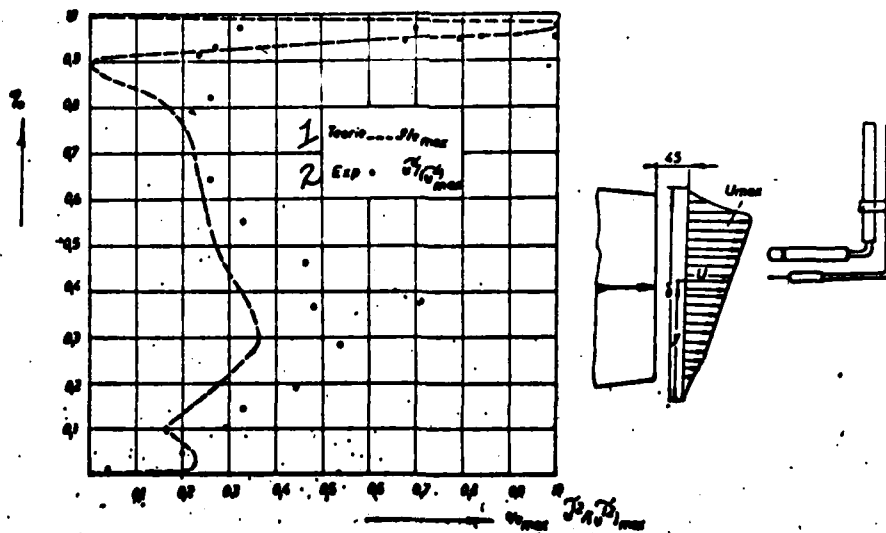


Figure 8-2.

Key: 1 - theory; 2 - experiment

TABLE 2

Measuring section	Roughness	Outside speed (working conditions of the wind tunnel)	Reynolds number $\frac{U_e x}{\nu}$	$\delta$ mm theoretic	$\delta$ mm experi- mental
CE $x = x_1$	normal	19.8	476,000	9.7	9.75
CE $x = x_2$	normal	19.8	1,180,000	20.2	20.4
tunnel $x = x_3$	normal	13.82	1,650,000	-	45
CE $x - x_1$	perturbator 5 mm = Dh	19.8	476,000	9.7	21.8
CE $x - x_2$	same	19.8	1,180,000	20.2	32

The experimental results are shown in Figure 8b and correspond to the experimental conditions presented in Table 2. The profiles in Figures 8a and 8c show the important modifications due to roughness, initially distributed in the form . The thickness can be evaluated theoretically by using the formula for a plane plate

$$\frac{\delta}{x} = 0,37 (R_x)^{-1/5}, \text{ and } R_x = \frac{U_e x}{\nu},$$

where the  $x$  origin for this wind tunnel was taken at  $x_0 = 0.056$  m upstream of the transition section from the collector to the straight segment of the perturbator zone  $P_1$  (Figure 8a). The presence of roughness  in zone  $P_1$  (it was obtained by shifting the frames in their guides by  $\Delta y = 5$  mm) increases the thickness of the boundary layer according to the formula:

$$\frac{\delta_r}{\delta} = F\left(\frac{\Delta y U_e}{\nu}\right)$$

where  $F$  is a universal function. We obtained  $\frac{\delta_r}{\delta} = 1,5 - 2$ . These results show that in the experimental chamber the usable zone (speed  $U_e = \text{const}$ ) represents approximately 80% of its cross-section, and that the artificial roughening of the walls allows at  $x = 3.17$  m

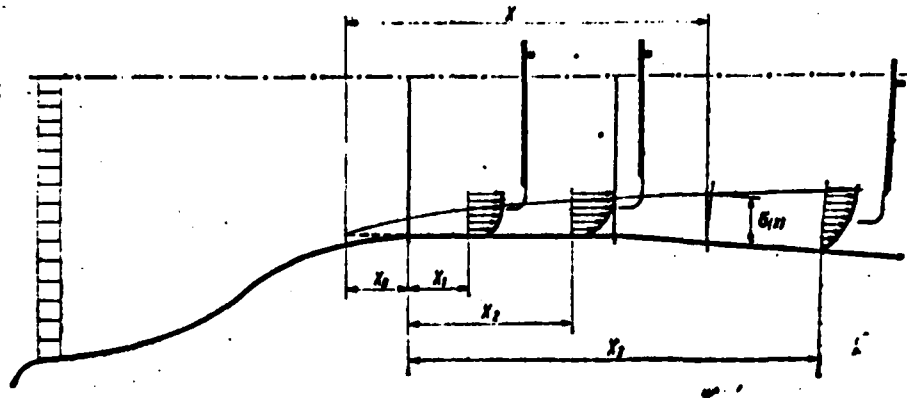


Figure 8a

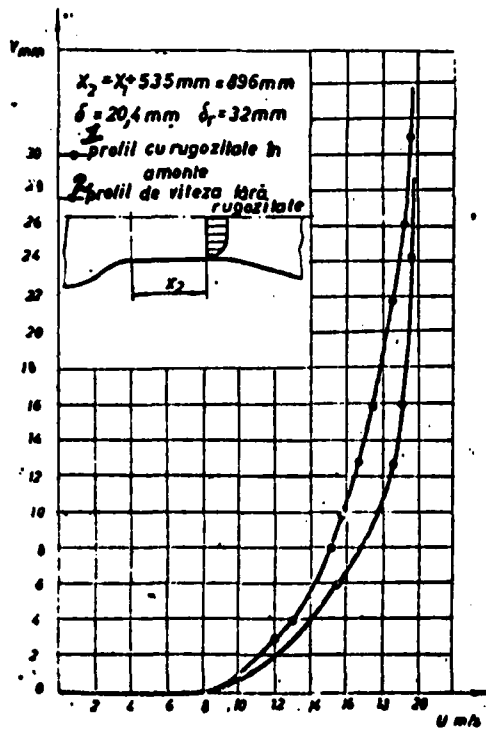


Figure 8b

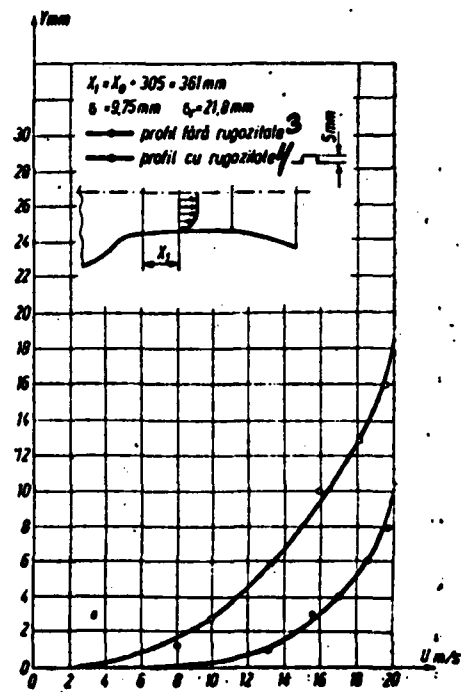


Figure 8c

Key: 1 - profile with roughness upstream; 2 - speed profile without roughness; 3 - profile without roughness; 4 - profile with roughness.

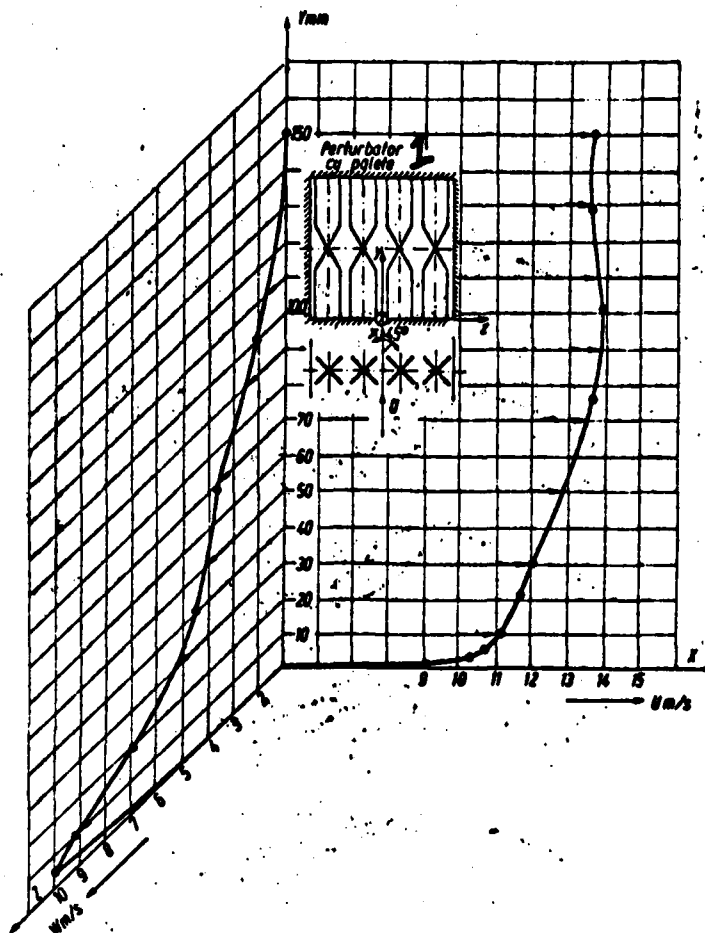


Figure 9

Key: 1 - perturbator with blades  
 (an eventual lengthening of the experimental chamber) with  $U_c = 10$  m/s to obtain  $\delta = 100$  mm.

Achieving certain speed profiles in the experimental zone. It is useful to indicate the possibilities offered by the perturbing systems, introduced in front of the two experimental zones, to achieve certain speed distributions at given sections. Thus in the experimental chamber a local three-dimensional behavior on a large scale of the boundary layer was simulated by creating a special speed profile. For this perturbators of the type  $\Delta$  were used, double blades on the same axis with their planes rotated at  $90^\circ$ . In Figure 9 are shown the three-dimensional speed profiles corresponding to

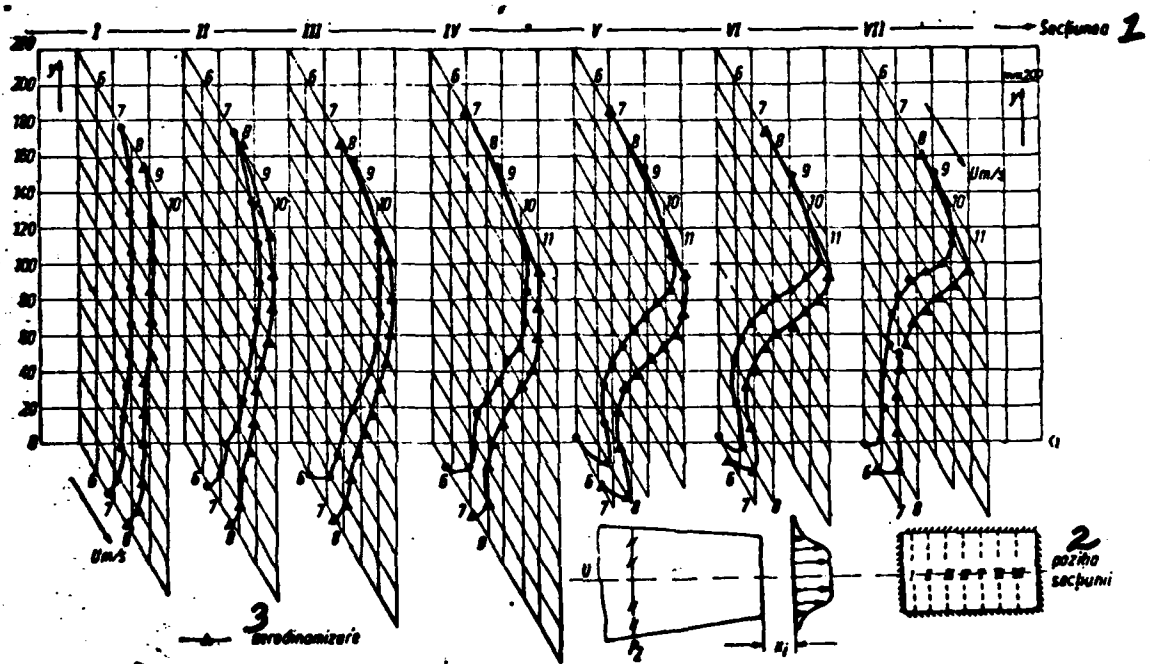


Figure 10.

Key: 1 - section; 2 - position of the section; 3 - aerodynamic.

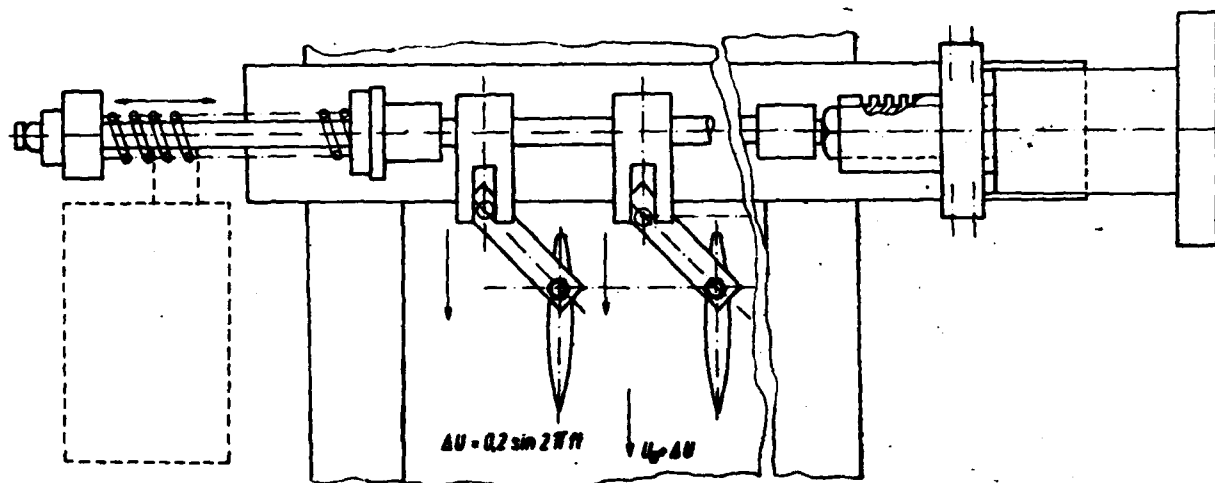


Figure 11.

the blades. They were obtained with a directional probe. They can serve for the study of the structure of the fluctuations as effected by three-dimensionality.

In the outgoing jet, due to the action of perturbator  $P_2$ , it is possible to obtain the desired speed distribution across 80% of the jet. In Figure 10 a series of speed profiles taken in seven sections of the outlet nozzle, at  $x_j = 20$  mm, with and without aerodynamic fan intake, are shown.

All these perturbators can serve to simulate flow in thick layers in which the speed profile plays an essential role, as for example in the atmospheric boundary layer. Finally we mention the possibility of obtaining flows with an oscillating character  $f = (2 - 5)$  Hz in the experimental chamber and in the outgoing jet, by using oscillating blades as perturbator  $P_1$ . The oscillatory motion of the blades is achieved through a motor, reducing gear and cam transmission to the blade axis. The kinematic scheme is shown in Figure 11.

## 5. Conclusion

We have presented the performance and technical characteristics of Eolin type wind tunnels, mainly as reference material for the users of this type of wind tunnel.

Secondly, we considered necessary a systematic study of the experimental possibilities offered by these wind tunnels for the solving of certain problems and finding new ones, as they occurred in various labs. They cover the range of flows at small speeds (2-20 m/s) and small and intermediate Reynolds numbers ( $10^3$ - $10^4$ ) for a reference length of 90 mm.

The occurrence of blocking effects enables the study of special internal flows or the introduction of larger models up to 50% of the section of the experimental chamber.

Finally, this type of wind tunnel is susceptible of modifications for special purposes (decreasing the degree of turbulence, controlling the boundary layer on the walls, creating of a longer collector as experimental segment, soundproofing of the fan chamber, etc.) and could be the starting point for designing of a similar wind tunnel on a large scale.

Received at redaction on 22 June, 1977

#### REFERENCES

1. V. TOMA, C. CRISTEA, ST. SĂVULESCU, *Cercetări experimentale asupra realizării unui jet cu gradient transversal constant al vitezei medii*, St. cerc. mec. apl., **34**, 2 (1975).
2. ST. N. SĂVULESCU, *The theory of fluctuating flow fields near Walls*, Part. 11, Rev. roum. sci. techn.-Méc. appl., **18**, 6 (1973).
3. A. POPR. J. HARPER, *Low-Speed wind tunnel testing*, John Wiley & Sons, Inc., New York. (1966).

DISTRIBUTION LIST

DISTRIBUTION DIRECT TO RECIPIENT

<u>ORGANIZATION</u>	<u>MICROFICHE</u>	<u>ORGANIZATION</u>	<u>MICROFICHE</u>
A205 DMATC	1	E053 AF/INAKA	1
A210 DMAAC	2	E017 AF/RDXTR-W	1
B344 DIA/RDS-3C	9	E403 AFSC/INA	1
C043 USAMIIA	1	E404 AEDC	1
C509 BALLISTIC RES LABS	1	E408 AFWL	1
C510 AIR MOBILITY R&D LAB/FIO	1	E410 ADTC	1
C513 PICATINNY ARSENAL	1	FTD	
C535 AVIATION SYS COMD	1	CCN	1
C591 FSTC	5	ASD/FTD/NIIS	3
C619 MIA REDSTONE	1	NIA/PHS	1
D008 NISC	1	NIIS	2
H300 USAICE (USAREUR)	1		
P005 DOE	1		
P050 CIA/CRB/ADD/SD	2		
NAVORDSTA (50L)	1		
NASA/NST-44	1		
AFIT/LD	1		
ILL/Code L-389	1		
NSA/1213/TDL	2		